

https://dspace.org/

# Property and structural characterisation of Fe and FeNi bonded NbC cermets for high temperature wear applications

**Gerrard Peters; Deena Naidoo; Rodney Genga; Adam Shnier; S. Ngongo**

https://hdl.handle.net/10539/46167
WOS

Downloaded from a DSpace repository. https://dspace.org/

International Journal of Refractory Metals and Hard Materials 128 (2025) 107041

Contents lists available at ScienceDirect

International Journal of Refractory Metals and Hard Materials

journal homepage: www.elsevier.com/locate/IJRMHM

# Property and structural characterisation of Fe and FeNi bonded NbC cermets for high temperature wear applications

G. Peters [a,*], D. Naidoo [a], R.M. Genga [b,c], A. Shnier [d], S. Ngongo [e]

[a] School of Physics, University of the Witwatersrand, 2050, South Africa
[b] Academic Development Unit (ADU), University of the Witwatersrand, 2050, South Africa
[c] School of Mechanical, Industrial and Aeronautical Engineering, University of the Witwatersrand, 2050, South Africa
[d] School of Chemistry, University of the Witwatersrand, 2050, South Africa
[e] CHRTEM, Nelson Mandela University, 6031, South Africa

ARTICLE INFO

*Keywords:*
NbC cermets
NbC-Fe
NbC-FeNi
Mechanical properties
High temperature abrasion wear
Elastic properties
Mo2C additives
Lattice parameters
Microstructures
Density
Hardness
Fracture toughness
Fe binders
Alternate binders

ABSTRACT

NbC cermets containing 12 wt% Fe and FeNi metallic binders were produced by liquid phase sintering at 1390 °C together with 12 wt% Co and Ni binders for comparison. The cermets were also produced with the addition of 0.4 wt% molybdenum carbide with the aim of improving the hardness property. Mechanical property measurements such hardness, toughness, and elastic properties were conducted on the materials, and these results indicate that the addition of molybdenum carbide improves the hardness with little compromise in the fracture toughness of the NbC cermets. The NbC-Fe cermet has the lowest Young's modulus value of 346 GPa, compared to 428 GPa and 462 GPa for the Co and Ni binder cermets, respectively. The microstructure and thermodynamics of the cermets were characterised using scanning transmission electron microscopy and X-ray diffraction. The microscopy results indicate that molybdenum carbide forms a solid solution in both the NbC hard phase and metal binder phase. No mixed metal carbides were observed in the samples with molybdenum carbide additions. X-ray diffraction results show a decrease in the NbC lattice parameter with the addition of $Mo_2C$ which is attributed to the formation of a mixed carbide phase, (Nb,Mo)C. High temperature dry sliding wear results reveal that the NbC cermets containing Fe and a 70/30 ratio of FeNi have the lowest wear rates at 700 °C, compared to Co and Ni binders. However, the $Mo_2C$ additions to the various binder NbC grades has an adverse effect on the high temperature wear rates. All the NbC grades with molybdenum carbide additions show an increase in the wear rate at 700 °C.

## 1. Introduction

WC-Co cermets continues to be the preferred choice of hardmetal due to its combination of good mechanical properties and wear resistance. However, factors such as cost, availability and toxicology regulations are driving research efforts to explore alternate materials such as niobium carbide based cermets [1]. Niobium carbide (NbC) has a high melting point (3520 °C), lower density (7.81 g/cm$^3$) compared to WC. Additionally, NbC has a lower Young's modulus (380–480 GPa) which results in reduced thermal stresses between the hard phase and metallic binder. Niobium carbide has good potential as an alternate hard phase due to its chemical stability, low density and high hardness at elevated temperatures [2,3]. Although Co has good wetting and solubility with WC, its poor high temperature properties result in rapid degradation during high-speed machining operations. Rapid softening of WC-Co hardmetals occurs at temperatures above 600 °C [4], and temperatures can reach above 1000 °C at the cutting edge during machining operations [5] resulting tool degradation. Cobalt is also toxic and can be subject to significant price fluctuations and availability [6]. Metal binders such as Fe and Ni have been identified as suitable replacements for Co, however, the alternate binders require further development to compete with the application and production advantages of Co binders [7].

Niobium carbide cermets with Co, Ni and Fe based binders have been investigated, and thus far, the NbC-Ni cermets with secondary carbides have exhibited a good combination of hardness and toughness properties [8]. Remarkable NbC grain growth is observed in Co and Ni binders after liquid phase sintering [9,10]. Transition metal carbide additives

* Corresponding author.
*E-mail address:* gerrard.peters@wits.ac.za (G. Peters).

https://doi.org/10.1016/j.ijrmhm.2025.107041
Received 14 October 2024; Received in revised form 23 December 2024; Accepted 2 January 2025
Available online 3 January 2025
0263-4368/© 2025 The Author(s). Published by Elsevier Ltd. This is an open access article under the CC BY license (http://creativecommons.org/licenses/by/4.0/).

such as VC, TiC, WC and $Mo_2C$ were reported to be efficient in the control of the microstructure of NbC-Co and NbC-Ni cermets by improving the densification and controlling NbC grain growth [10]. Studies of NbC-Ni cermets with $Mo_2C$ additions have shown that the hardness increases whereas the toughness decreases, which was ascribed to variations of the carbide grain size and the higher solute content in the binder [1,6]. Woydt et al. [11] reported that $NbC_{0.88}$-12Co has a similar hot hardness as WC cemented carbides at 600 °C, and a higher hot hardness at 700 °C. At room temperature the wear rates of NbC cermets were low and less sensitive to increasing sliding speed, and at 400 °C the wear rates generally remained low [12].

The properties of NbC, together with stable high temperature elastic moduli and hardness make the NbC cermets suitable for high temperature wear and cutting applications [13,14]. In this study, the effect of $Mo_2C$ additives on the microstructure and mechanical properties of Fe based NbC cermets are evaluated, as well as the performance of the Fe based NbC cermets in dry sliding wear at 700 °C.

## 2. Experimental

### 2.1. Materials preparation

The powders used to produce the composites had a nominal starting grain size of 1 μm, except for the WC which had a starting grain size of 0.8 μm. The composites were produced with 12 wt% metal binders and the compositions of the different grades are summarised in Table 1. In the NbC-FeNi grade, the ratio of the metallic binder is 70/30 (Fe/Ni) to maintain an austenitic structure after sintering [15]. The powder mixtures were wet milled in a stainless steel pot using a laboratory scale ball mill. Powder batches of 100 g each were prepared using the nominal compositions given in Table 2. The powders were milled together with 40 g ethanol and 2 wt% polyethylene glycol (PEG) for 24 h at a speed of 140 rpm. Sintered WC-6Co pellets was used as the milling media in a 5:1 ball-to-powder ratio. The milled mixtures were dried, screened through a 120 μm sieve, and pressed into green compacts at a pressure of 140 MPa. The size of pressed compacts were approximately 12 × 12 mm square, and a thickness of 6 mm. Larger components (40 mm diameter and 4 mm thickness) were pressed for the high temperature dry sliding wear tests.

The green compacts were liquid phase sintered using an ULTRA-TEMP SinterHIP furnace at Pilot Tools (PTY) LTD. Standard cemented carbide production sintering cycles were used for sintering of test pieces at 1360 °C, 1390 °C and 1430 °C, and based on their microstructures, hardness and density measurements, 1390 °C was selected as the sintering temperature for the cermet grades in this study. The initial stage of the sintering cycle included dewaxing or removal of the PEG at a temperature range between 270 °C and 450 °C in H2-atmosphere. After dewaxing, the furnace is heated under vacuum to 1000 °C where a carbon correction procedure was performed for 2 h using a mixture of hydrogen and methane gasses. Thereafter, the furnace was heated under vacuum at 2.4 °C/min to 1200 °C. A cobalt loss protection (CLP) was carried out at 1200 °C using argon gas at a pressure of 0.37 MPa. The furnace was heated under vacuum at a rate of 3.5 °C/min to the sintering temperature where the temperature was held constant for 90 min. This was followed by hot isostatic pressing (HIP) which was carried out at the sintering temperature for 20 min under argon atmosphere at a pressure of 4.4 MPa.

**Table 1**
Nominal compositions given in wt% for the different cermet grades.

| Cermet grade | NbC (1 μm) | WC (0.8 μm) | $Mo_2C$ (1 μm) | Co (1 μm) | Fe (1 μm) | Ni (1 μm) |
|---|---|---|---|---|---|---|
| NbC-Co | 88 | | | 12 | | |
| NbC-Co + Mo2C | 84 | | 4 | 12 | | |
| NbC-Fe | 88 | | | | 12 | |
| NbC-Fe + Mo2C | 84 | | 4 | | 12 | |
| NbC-FeNi | 88 | | | | 8.4 | 3.6 |
| NbC-FeNi + Mo2C | 84 | | 4 | | 8.4 | 3.6 |
| NbC-Ni | 88 | | | | | 12 |
| NbC-Ni + Mo2C | 84 | | 4 | | | 12 |
| WC-Co | | 88 | | 12 | | |
| WC-Co + Mo2C | | 84 | 4 | 12 | | |

**Table 2**
Density, porosity and mean carbide grain size for the cermet grades sintered at 1390 °C.

| Sample | Measured Density ($g/cm^3$) | % Densification | Apparent Porosity | Mean Carbide Grain Size (μm) |
|---|---|---|---|---|
| WC-12Co | 14.29 | 100.35 | A02 | 1.07 ± 0.04 |
| WC-12Co + $4Mo_2C$ | 13.94 | 99.64 | A02 | 0.71 ± 0.02 |
| NbC-12Co | 7.87 | 99.12 | A06 + B06 | 6.92 ± 0.32 |
| NbC-12Co + $4Mo_2C$ | 7.93 | 99.50 | A06 | 4.70 ± 0.60 |
| NbC-12Fe | 7.75 | 99.10 | A08 | 6.24 ± 0.20 |
| NbC-12Fe + $4Mo_2C$ | 7.82 | 99.59 | A06 | 6.72 ± 0.64 |
| NbC-12FeNi | 7.79 | 99.24 | A08 | 6.40 ± 0.22 |
| NbC-12FeNi + $4Mo_2C$ | 7.84 | 99.62 | A06 | 5.07 ± 0.08 |
| NbC-12Ni | 7.87 | 99.12 | A08 + B04 | 7.28 ± 0.16 |
| NbC-12Ni + $4Mo_2C$ | 7.92 | 99.50 | A06 | 3.46 ± 0.35 |

### 2.2. Materials characterisation

The densities of the sintered materials were measured with a SHIMADZU AY120 density balance based on the Archimedes principle. Evaluation of the apparent porosity was determined using a Zeiss AX10 metallurgical microscope. The porosity size and distributions were classified according to the ISO 4499-4 international standard for hardmetals. Vickers hardness ($HV_{30}$) measurements were undertaken utilising a load of 30 kg on polished cross sections. The Palmqvist fracture toughness ($K_{IC}$) was measured using the Shetty equation on the crack lengths of the hardness indentations. The results were calculated using an average of five indentations. The elastic and shear modulus were obtained using a 45MG Olympus ultrasonic thickness gauge. The velocity of sound was measured in the shear and longitudinal directions to calculate the elastic properties.

The microstructures of the cermets were examined using a Zeiss SIGMA field emission scanning electron microscope (FE-SEM). A JEOL 2100 scanning transmission electron microscope (STEM) was used for elemental mapping on focused ion beam sections (FIB) of the different phases in the materials. The carbide grain size was determined using ImageJ software on five randomly selected areas for each sample. The magnifications were varied for each grade to ensure that a minimum of at least 400 grains were measured in accordance with the National Physical Laboratory (NPL) measurement good practice guide No. 21 [16]. The grain size was determined by measuring the Feret diameters of the carbide grains [17]. X-ray diffraction (XRD) measurements were carried out using a Bruker D2 Phaser equipped with a Co radiation source with a Fe $K_\beta$ filter. The XRD measurements were performed on the milled powders and sintered components, with the lattice parameters calculated using Rietveld refinement in the Bruker TOPAS software.

High temperature dry sliding abrasion tests were undertaken using a ball-on-disc tribometer at BAM, Germany. The test procedure complies with ASTM G99 and DIN EN 1071–13:2010 [18]. The high temperature abrasion tests were performed at 700 °C with an applied force of 10 N, and a sliding speed of 1.17 m/s for a distance of 500 m using alumina balls. A HOMMEL T8000 tactile roughness tester was used to measure the samples' worn volumes ($\Delta V_S$) using the wear formula in eq. 1.

$$\Delta V_s = (\pi R(S1 + S2 + S3 + S4))/2 \quad (1)$$

where R is the sliding radius and S is the planimetric worn track cross sectional area.

The worn volumes of the samples were used to calculate the samples' wear rate (SWR) using the equation below [19].

$$SWR = \Delta V_s / F.s \quad (2)$$

where F is the applied force (N), and s is the sliding distance (m).

## 3. Results and discussion

### 3.1. Microstructure

The microstructures of the various metal binder NbC cermets sintered at 1360 °C without the $Mo_2C$ additive show high levels of porosity and poor metal binder distribution indicating that the sintering temperature was too low to achieve full density. The addition of $Mo_2C$ to the various binder cermets show much reduced porosity levels and an improvement in the binder distribution in all the grades sintered at 1360 °C. The microstructures of NbC-Fe and NbC-Fe + $Mo_2C$ grades sintered at 1360 °C shown in Fig. 1 illustrates the improvement in density from 92.2 % for the NbC-Fe (Fig. 1a) to 99.4 % for NbC-Fe-$Mo_2C$ grade, respectively (Fig. 1b). This indicates that $Mo_2C$ acts as a sintering aid. Huang et al. [20] reported $Mo_2C$and VC additives act as a sintering aid between the hard phase (NbC) and metal binder as the formation enthalpy ($\Delta H_f$) of $Mo_2C$ (17.6 KJ/mol) is much lower than NbC (143 KJ/mol), thereby providing better wettability between the metal and carbide phases. The NbC cermets sintered at 1390 °C have acceptable microstructures even though minor porosity was observed. The densities for the various cermet grades sintered at 1390 °C were greater than 99 % as recorded in Table 2. Examination of the microstructures show A02 porosity present in the WC grades, whilst the porosity of the NbC grades vary between A06 and A08 (Table 2), with B type porosity only present in the NbC-Co and NbC-Ni grades. At 1430 °C, the microstructures of the NbC-Co and NbC-Ni grades without the $Mo_2C$ additive showed severe NbC grain growth indicative of the sintering temperature being too high for these NbC grades. Therefore, 1390 °C was selected as the sintering temperature for materials characterisation.

The NbC grains coarsen significantly during liquid phase sintering with the mean carbide grain size increasing from the nominal grain size of 1 μm, to 6–7 μm for the all the NbC cermet grades sintered at 1390 °C (Table 2). Grain growth occurs due to the Oswald ripening process because of the difference between grains of dissimilar sizes [21]. The mechanisms of grain growth are described as diffusion-control of atoms in a metal matrix, and through reaction-control of atoms at a solid/liquid interface. The metal binders also have poor wettability with NbC grains [20], and together with the low solubility of NbC in the metal binders result in the grain coarsening. The solubility of NbC in Fe, and Ni and Co is 1, 3 and 5 wt%, respectively at 1250 °C [22]. In contrast to the NbC grades, the mean sintered carbide grain size of the WC-Co grade (1.07 μm) increases marginally from the nominal starting grain size (0.80 μm) at the sintering temperature of 1390 °C, and the addition of $Mo_2C$ reduces the WC grain size to 0.71 μm.

The addition of $Mo_2C$ has a substantial effect in reducing the carbide grain size of the NbC-Co and NbC-Ni binder cermets. The biggest influence of the $Mo_2C$ additive was observed for the NbC-Ni grade, where the sintered carbide grain size was reduced from 7.28 ± 0.16 to 3.46 ± 0.35 μm. The backscattered electron images (BSE) showing the effect of $Mo_2C$ on the microstructures of the NbC-Ni grade are shown in Figs. 2(a) and 2(b). For the NbC-Fe cermet, the addition of $Mo_2C$ has a negligible influence on the carbide grain size. The mean carbide grain size was measured as 6.24 ± 0.20 μm for the NbC-Fe grade and 6.74 ± 0.64 μm for the NbC-Fe-$Mo_2C$ grade. The carbide grain size for the NbC-FeNi grade is reduced from 6.40 ± 0.22 to 5.07 ± 0.08 with the $Mo_2C$ additive. In WC hardmetals, Wittmann et al. [23] showed that the Fe binder in a WC-10wt%Fe acts as a grain growth inhibitor without additives, in comparison to WC-10wt%Ni which has strong grain growth. This effect was interpreted as the ability of iron to form stable metal-carbon bonds, with the iron masking the carbon, and by increasing the activation energies of the nucleation and growth processes impeding carbon transport and precipitation. Niobium carbide grain growth, however, is observed in the NbC-Fe bonded cermets (Fe and FeNi) which is less than the grain growth observed for the Co and Ni binder NbC cermets as indicated by the measured grain sizes in Table 2. A change in the morphology of the carbide grains is observed in the NbC-Fe grade with the addition of $Mo_2C$, from irregular and angular shape to a more rounded carbide structure as shown in Figs. 2(c) and 2(d). The morphology of the carbide grains for the NbC cermet grades with Co, FeNi and Ni binders with 0.4 wt% $Mo_2C$ additive consisted of more irregular and angular shaped carbide grains. Huang et al. [24] also observed well faceted large grains with smaller spherical grains in NbC-12vol%Fe, and irregular shaped grains for Co and Ni binders which was attributed to the surface energies of the metal binder influencing the wetting angle.

Elemental X-ray mapping was conducted on FIB sections of grades sintered at 1390 °C for determining the phase compositions in the different cermet grades. The addition of $Mo_2C$ to the reference WC-Co grade results in the formation of eta phase (η-phase), Co-W-Mo-C. In WC-Co systems with low carbon content, the binary phase diagram indicates the formation of two types of eta phase, $M_6C$ and $M_{12}C$, which

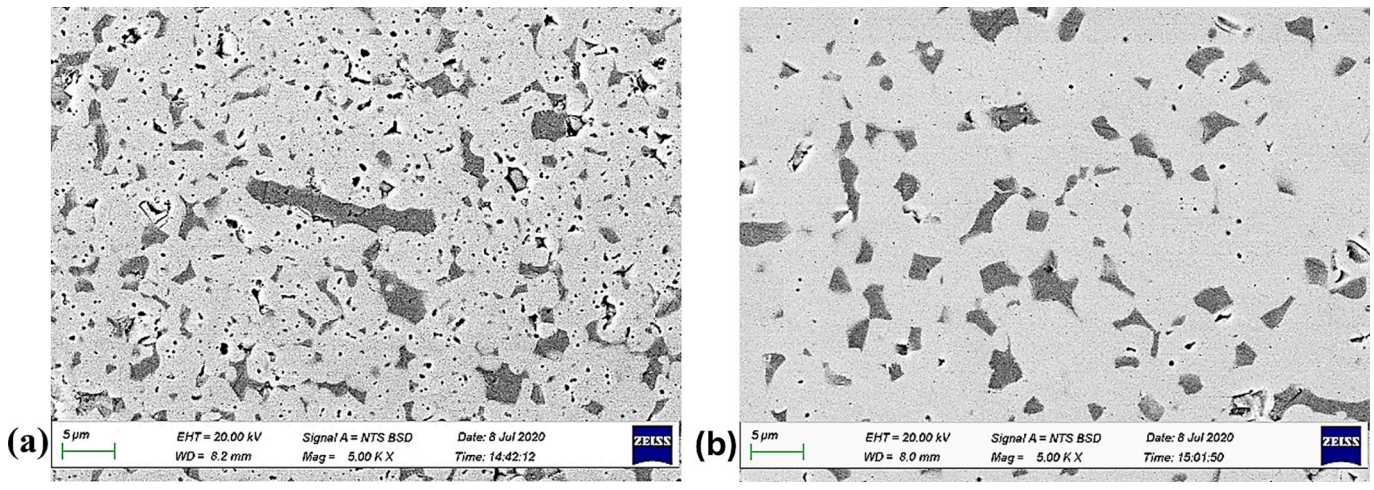



**Fig. 1.** BSE images showing the effect of $Mo_2C$ additions in the Ni and Fe binder cermets; (a) NbC-Ni, (b) NbC-Ni-$Mo_2C$, (c) NbC-Fe and (d) NbC-Fe-$Mo_2C$.

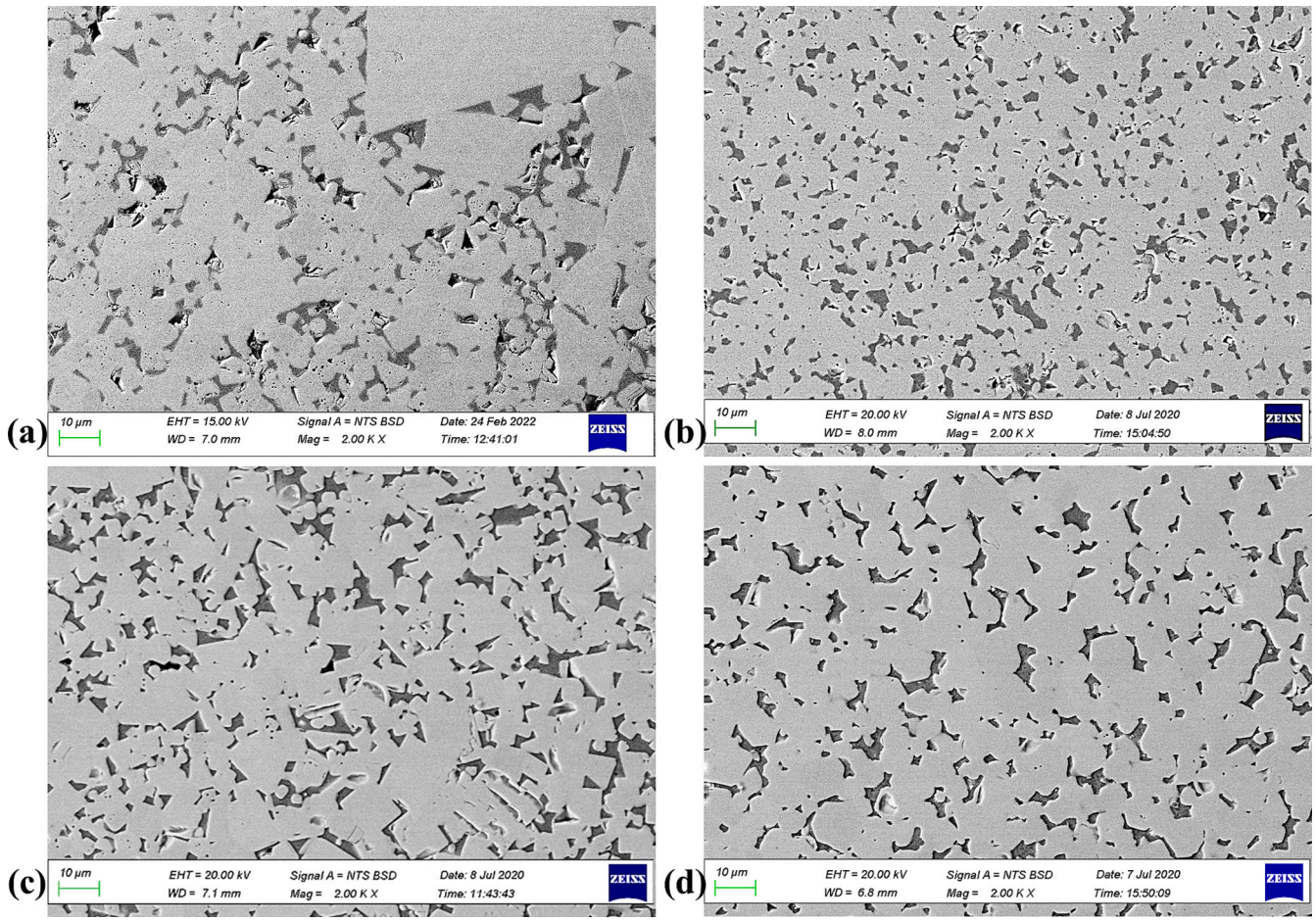



**Fig. 2.** BSE images showing the effect of $Mo_2C$ additions in the Ni and Fe binder cermets; (a) NbC-Ni, (b) NbC-Ni-$Mo_2C$, (c) NbC-Fe and (d) NbC-Fe-$Mo_2C$.

are namely $Co_3W_3C$ and $Co_6W_6C$ phases [25,26]. However, Li et al. [27] illustrated that Mo significantly promotes the formation of eta phase, and that the Mo is mainly concentrated in the η-phase particles. Hence, the presence of η-phase observed in the WC-Co-$Mo_2C$ grade is due to presence of Mo and not low carbon concentrations. The distribution of Mo in the η-phase determined by elemental X-ray mapping is shown in Fig. 3.

In all the NbC grades with the different metal binders (Co, Fe and FeNi), the addition of $Mo_2C$ forms a solid solution with NbC hard phase and metal binder phases. An example of the NbC-FeNi grade showing the dispersion of $Mo_2C$ in the NbC and FeNi phases is given in Fig. 4. Similar observations were made for the Co, Fe and Ni binder NbC cermets where the $Mo_2C$ formed a solid solution with the NbC and metal binder. Labonne et al. [6] reported that $Mo_2C$ almost completely dissolves during the solid-state sintering stage between 1080 °C and 1180 °C in both the NbC hard phase and Ni binder.

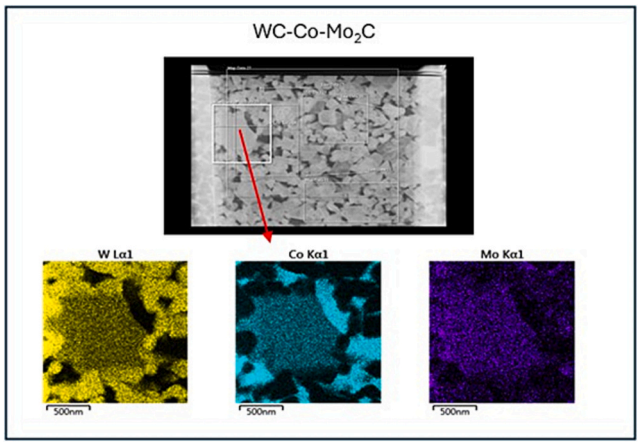



**Fig. 3.** X-ray maps of the eta-phase observed in the WC-Co-$Mo_2C$ grade.

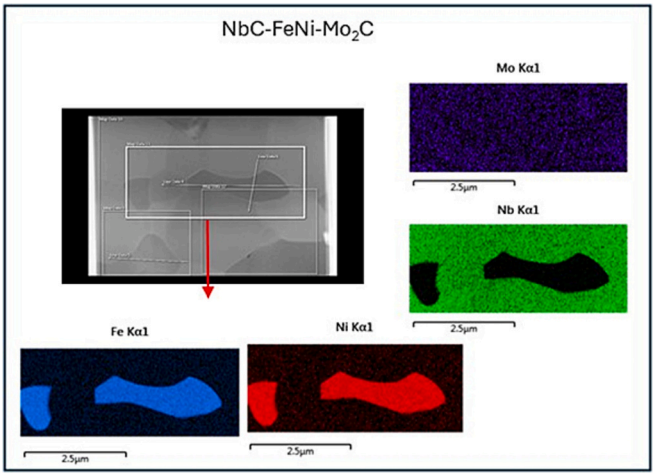



**Fig. 4.** X-ray maps showing the dispersion of $Mo_2C$ in the NbC and FeNi phases.

### 3.2. X-ray diffraction

X-ray diffraction results for the sintered cermets without the $Mo_2C$ additive are consistent with the nominal compositions for the different grades. The addition of $Mo_2C$ formation of results in the formation of a solid solution of the $Mo_2C$ with the NbC hard phase and the metal binder for all the NbC cermet grades forming a mixed carbide,(Nb,Mo)C. The $Mo_2C$ phase is observed in the milled powders, and not in the sintered NbC components which consists of a two-phase microstructure as shown in Fig. 5. This is corroborated by the STEM X-ray mapping observations shown in Fig. 4. The XRD results are consistent with the work by Huang et al. [1] who identified only a Ni alloyed binder and a (Nb,Mo)C solid solution in NbC-Ni doped with $Mo_2C$.

The XRD pattern of the WC-Co show the formation of η-phase the addition of $Mo_2C$ as shown in Fig. 6. The lattice constants for WC and the η-phase are similar, indicating that the addition of Mo and C does not cause a large lattice strain. The atomic radii of W and Mo are 1.37 Å and 1.36 Å, respectively, therefore, the substitution of Mo in a W lattice will not produce large lattice strain [27].

The measured lattice parameters for the NbC phase show a decrease in the lattice parameter with the addition of $Mo_2C$ (Fig. 7). The decrease in the unit cell is probably due to the smaller atomic radius of Mo (139 pm) compared to Nb (146 pm) [28]. The observations are consistent with work on NbC-Ni cermets with $Mo_2C$ additions reported by Labonne et al. [6] which showed a decrease in the NbC lattice parameter with the addition of $Mo_2C$, and an increase in the Ni lattice parameter. Thus, indicating that $Mo_2C$ dissolves in the NbC and Ni binder resulting in a smaller unit cell for the mixed carbide compared to the NbC reference phase or starting raw NbC powder.

### 3.3. Mechanical properties

The Vickers hardness for the various cermet grades is shown graphically in Fig. 8. The hardness of the NbC-Fe cermet (12.25 GPa) is higher than the NbC cermets containing Co, FeNi and Ni binders which have hardness values of 11.00 GPa, 11.45 GPa and 10.67 GPa, respectively (Table 3). Iron has a high affinity for carbon compared to Co and Ni [29] which is likely to promote increased hardness. Huang et al. [24] also reported that Fe based binders have a higher hardness than Co and Ni based NbC cermets. The addition of $Mo_2C$ has a significant improvement in hardness across all the binder grades.

In hardmetals, there is a Hall-Petch relationship between hardness and grain size [16], where hardness $\propto$ (grain size)$^{-½}$. Finer carbide structures exhibit higher hardness and lower fracture toughness [30]

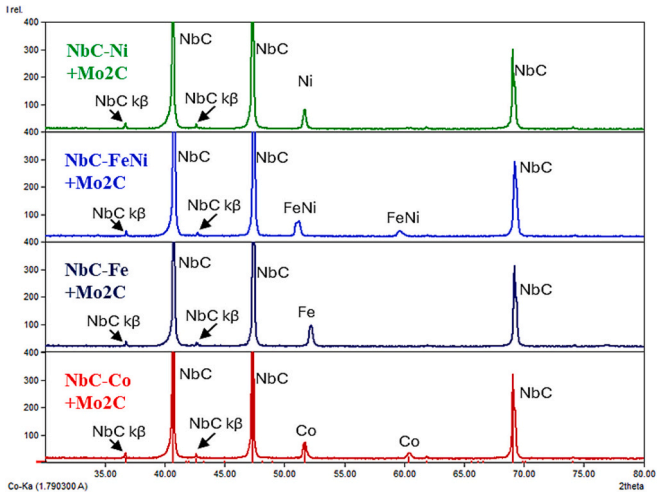



**Fig. 5.** XRD patterns of NbC cermets sintered at 1390 °C with $Mo_2C$ additives showing a two-phase structure.

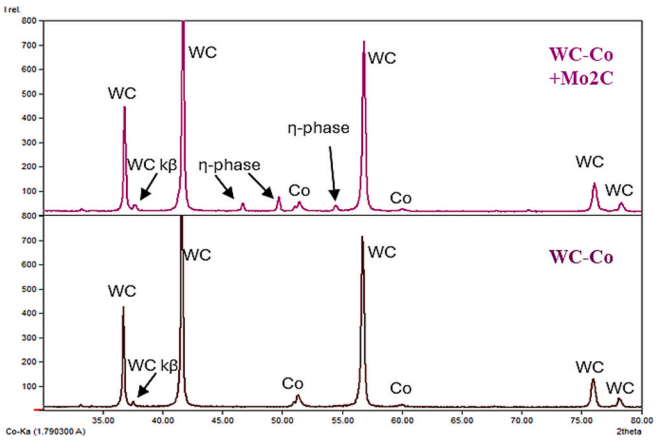



**Fig. 6.** XRD patterns of the WC-12Co grades.

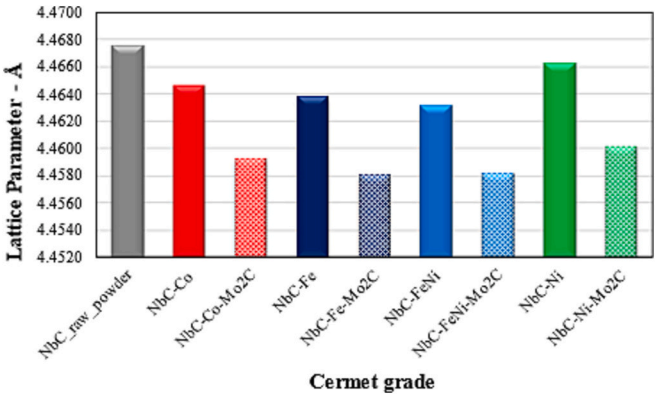



**Fig. 7.** Effect of $Mo_2C$ additions on the NbC lattice parameters.

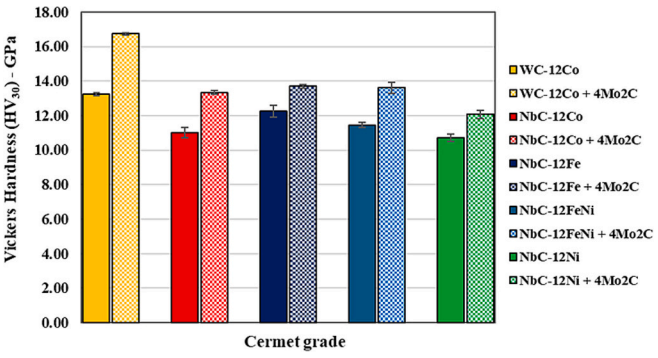



**Fig. 8.** Vickers hardness ($HV_{30}$) for the different cermet grades.

than coarser microstructures due to the increase in carbide volume. The Hall-Petch relationship is well known in conventional hardmetals and binderless WC [31]. In NbC cermets containing $Mo_2C$ additives, Pötschke et al. [31] studied the influence of the addition of secondary carbides, VC and $Mo_2C$, to binderless NbC produced using SinterHIP and spark plasma sintering (SPS). A larger carbide grain size was observed in the NbC-10vol%$Mo_2C$ sample produced using SinterHIP compared to the same material produced by SPS. The hardness of the SinterHIP sample (1900 $HV_{10}$) was 250 HV higher than the sample produced by SPS with a finer grain structure. Pötschke et al. [31] attributed the increase in hardness to solid solution strengthening due to the formation of the mixed carbide, (Nb,Mo)C. The improvement in the hardness of the NbC cermets with $Mo_2C$ additions can therefore be attributed to a

**Table 3**
Mechanical properties of the NbC cermets.

| Grade | $HV_{30}$ (GPa) | $K_{IC}$ (MPa.$m^{1/2}$) | Elastic Modulus (GPa) | Shear Modulus (GPa) |
|---|---|---|---|---|
| WC-12Co | 13.23 ± 0.07 | 13.30 ± 0.23 | 545 ± 3 | 223 ± 1 |
| WC-12Co + 4Mo2C | 16.74 ± 0.06 | 10.48 ± 0.14 | 530 ± 1 | 213 ± 1 |
| NbC-12Co | 11.00 ± 0.31 | 10.82 ± 0.80 | 428 ± 3 | 177 ± 2 |
| NbC-12Co + 4Mo2C | 13.34 ± 0.09 | 8.58 ± 0.73 | 381 ± 3 | 160 ± 1 |
| NbC-12Fe | 12.25 ± 0.35 | 6.66 ± 0.25 | 346 ± 6 | 147 ± 5 |
| NbC-12Fe + 4Mo2C | 13.69 ± 0.09 | 6.69 ± 0.32 | 350 ± 2 | 148 ± 1 |
| NbC-12FeNi | 11.45 ± 0.16 | 6.58 ± 0.34 | 403 ± 1 | 165 ± 1 |
| NbC-12FeNi + 4Mo2C | 13.60 ± 0.32 | 6.72 ± 0.29 | 393 ± 4 | 162 ± 3 |
| NbC-12Ni | 10.67 ± 0.22 | 15.21 ± 0.82 | 462 ± 5 | 193 ± 3 |
| NbC-12Ni + 4Mo2C | 12.06 ± 0.23 | 14.37 ± 0.74 | 410 ± 1 | 169 ± 1 |

combination of finer carbide structures and solid solution strengthening due to the formation of the mixed carbide phase (Nb,Mo)C.

The WC-Co grade which has the lowest sintered grain size of 1.07 μm (Table 2), has the highest hardness value of 13.23 ± 0.07 GPa as shown in Table 3. The addition of $Mo_2C$ to the WC-Co grade further increases the hardness from 13.23 ± 0.07 GPa to 16.74 ± 0.06 GPa (Table 3). A decrease in the fracture toughness property from 13.3 MPa.$m^{1/2}$ to 10.48 MPa.$m^{1/2}$ is observed with the $Mo_2C$ addition. For the NbC cermets, the fracture toughness of the Fe based binders (Fe and FeNi) are lower than the Co and Ni binder systems. The Ni binder grade has the lowest hardness and highest fracture toughness value probably due to the larger grain size (7.28 μm) which would indicate a larger binder pool size. Also, the higher stacking fault energy of Ni (125 mJ/$m^2$) compared to Co (20 mJ/$m^2$), results in a moderate work hardening of Ni [7]. Therefore, in WC hardmetals, the hardness and strength of WC-Co tends to be superior to WC-Ni [32].

Comparable hardness and toughness data plots of the NbC cermets are presented in Fig. 9. The materials in this study are compared to some WC-based hardmetals [33], NbC-based cermets [24,28,34] and TiCN-based cermets [35]. The comparative materials were all produced by conventional sintering (liquid phase sintering) techniques having similar binder contents where possible. The grain size of the hard phase however, are not similar.

The Fe based binders (Fe and FeNi) have lower elastic (Young's modulus) and shear modulus values compared to the NbC cermets with Co and Ni binders (Table 3). The lower elastic properties values indicate that the thermal stresses induced by NbC, and metal binder will be lower in comparison to WC [8]. Woydt et al. [3] reported that this trend can be explained in terms of the larger coefficient of thermal expansion of NbC is closer to that of typical binder metals as well as the lower Young's Modulus of NbC will have a reduced mismatch. The addition of $Mo_2C$ to the Fe based binders (Fe and FeNi) has a minimal effect on the elastic properties, whereas, for the Co and Ni binders, the $Mo_2C$ additive reduces the elastic properties. As the elastic modulus is independent of grain size, and the densities are greater than 99 %, the reduced elastic modulus could be due to the lower bonding strength between NbC, $Mo_2C$ and the metal binder [36]. The higher activation energies of the nucleation and growth processes and the strong metal-carbon bonds in the Fe binder systems [23], could explain the lower elastic modulus for the NbC cermets with Fe binders. However, the minor porosity observed in the NbC grades would result in lower elastic modulus values for all the NbC cermet grades.

### 3.4. High temperature sliding wear

In the high temperature dry sliding wear test, the NbC cermets containing Fe and FeNi showed the lowest sample wear rates at 700 °C compared to the Co and Ni binders (Fig. 10). The wear rates of the NbC-Fe and NbC-FeNi grades are also significantly lower than WC-Co. The

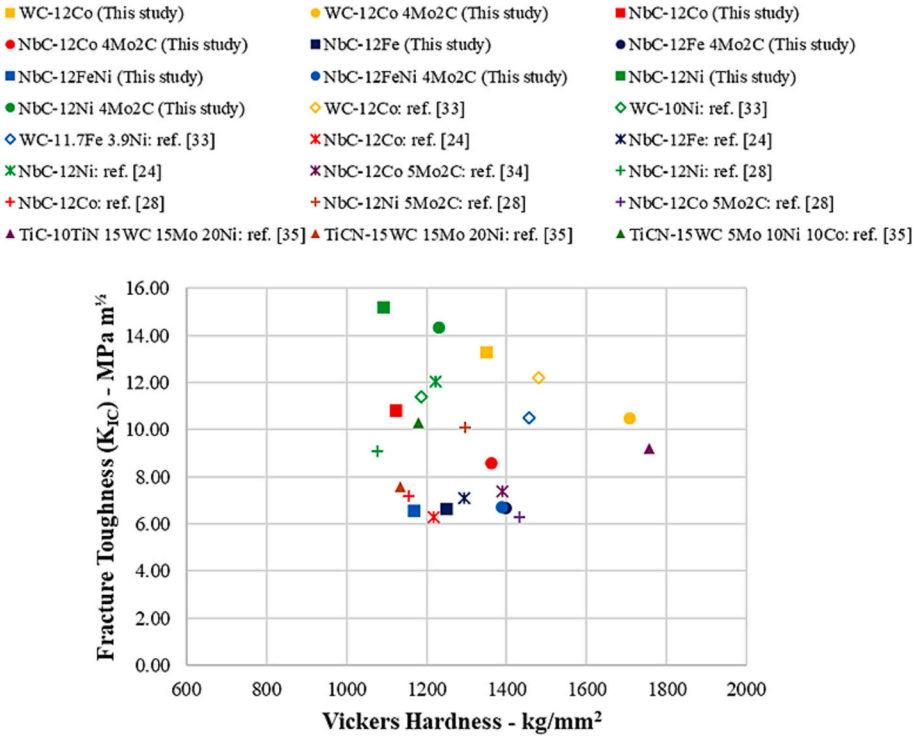



**Fig. 9.** Hardness and fracture toughness properties compared to literature data [24,28,33–35].

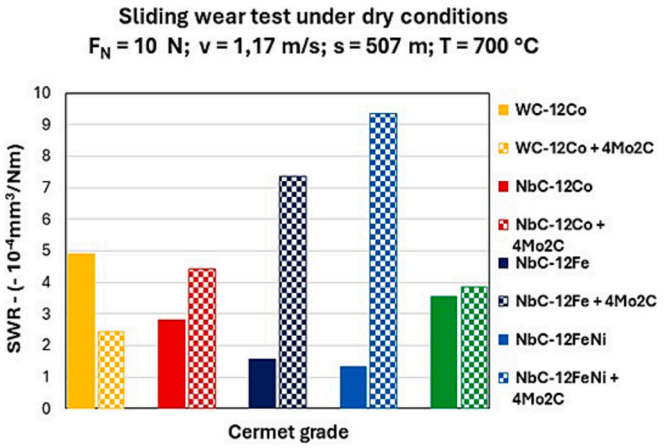



**Fig. 10.** Sample Wear Rates for the cermets grades at 700 °C.

addition of $Mo_2C$ to the NbC cermets increases the samples' wear rates, especially in the Fe based NbC grades (Table 4). In WC-Co, however, the addition of $Mo_2C$ lowers the wear rate. This could be due to the η-phase formation in these materials together with the much finer grain structure, whilst in the NbC grades, the $Mo_2C$ additives form a solid solution with the NbC resulting in a mixed carbide, (Nb,Mo)C.

Genga et al. [36] reported a similar trend in dry sliding wear tests at 400 °C for liquid phase sintered NbC-12Ni cermets, where the addition of $Mo_2C$ resulted in an increase in the wear rate of the material. The SWR increased from $3.56 \times 10^{-6}$ mm³/Nm to $8.47 \times 10^{-6}$ mm³/Nm with the addition of $Mo_2C$ to the NbC-12Ni cermet. At 400 °C, WC-10Co had the lowest SWR ($1.47 \times 10^{-6}$ mm³/Nm), suggesting that the high temperature benefits of NbC grades in dry sliding wear occur above 400 °C as all the NbC grades in Fig. 9 have lower wear rates than WC-Co at 700 °C.

The measured coefficient of friction ($\mu$) values shown in Table 4 are lower with the addition of $Mo_2C$. Only the NbC-Ni grade shows no change the coefficient of friction with the $Mo_2C$ additive. Genga et al. showed a similar observation for the coefficient of friction values for NbC-12wt%Ni (0.449) and NbC-$Mo_2C_x$-12wt%Ni (0.479) in dry sliding tests at 400 °C [36]. Woydt et al. [12] showed that in dry sliding tests, the friction of binderless NbC increased with increasing sliding distance at room temperature, and at 400 °C, the friction decreased in all the NbC grades including the binderless NbC, NbC-Ni, NbC-Co and NbC-$Fe_3Al$. Low friction is regarded as a favourable property for cutting tools as the cutting forces are reduced. The wear rates of Co binder NbC grades were lower than the Ni and $Fe_3Al$ binder cermets which was attributed to the formation of $Co_3O_4$ tribo-oxidation lowering the wear rate [18].The wear of ferrous (Fe based) materials under dry oscillation is dominated by the tribo-oxidative formation of $Fe_2O_3$ and/or α, $\beta$ or ɣ-FeOOH and Fe $(OH)_2$ at room temperature [12].

Tribo-oxidation or tribo-chemical wear is a chemical reaction that can lead to loss of material in tribo-contacts. NbC oxidises in air at increasing temperatures forming $Nb_2O_5$ and other block structure oxides ($Nb_{3n-1}O_{8n-2}$), and the rate of oxidation increases rapidly above 500 °C [37]. At 700 °C, NbC primarily oxides to $Nb_2O_5$ in NbC-Ni cermets [38]. The formation of $Nb_2O_5$ reduces friction and wear rates during dry sliding wear tests of NbC cermets [39]. Tribo-oxidatively formed $Nb_2O_5$ melts at 1512 °C and has a hardness between 500 and 650 $HV_{0.2}$ which contributes to the wear resistance [14,39]. Hadi et al. [40] showed that the addition of $Mo_2C$ reduced the oxidation resistance in (Ti,W)CN cermets. The study showed that the presence of W and Mo in the $TiO_2$ oxide layer caused brittleness, leading to spallation of the oxide layer. In a comparative study on the oxidation behaviour of cermets, Anwer et al. [41] reported that incorporation of $Mo_2C$ in a NbC-Ni based cermet significantly decreased the oxidation resistance at 700 °C, which was attributed to the evaporation of $MoO_3$, as $MoO_3$ becomes volatile above 600 °C [41,42]. It is possible that similar effects occur with $Mo_2C$ additives in the NbC cermets in this study leading to increased wear.

**Table 4**
Sample Wear rates and coefficient of friction values for the cermet grades.

| Grade | Sample Wear rate $10^{-4}$ mm³/Nm | Coefficient of Friction ($\mu$) |
|---|---|---|
| WC-12Co | 4.91 | 0.41 |
| WC-12Co + 4Mo2C | 2.44 | 0.35 |
| NbC-12Co | 2.82 | 0.46 |
| NbC-12Co + 4Mo2C | 4.41 | 0.42 |
| NbC-12Fe | 1.55 | 0.44 |
| NbC-12Fe + 4Mo2C | 7.37 | 0.40 |
| NbC-12FeNi | 1.32 | 0.45 |
| NbC-12FeNi + 4Mo2C | 9.34 | 0.40 |
| NbC-12Ni | 3.55 | 0.44 |
| NbC-12Ni + 4Mo2C | 3.85 | 0.45 |

## 4. Conclusions

The room temperature mechanical property results indicate that the NbC-12wt%Fe and NbC-12wt%FeNi have higher hardness values than the NbC-Co and NbC-Ni cermet grades. The WC-12wt%Co has the best combination of hardness and fracture toughness properties in comparison to the NbC cermets. The excellent properties of the WC-Co grade are mostly due to the much finer microstructure with a mean carbide grain size of 1.07 μm compared to the NbC sintered grain size of between 6 and 7 μm. The fracture toughness of the Fe based NbC cermets are significantly lower than the other binder grades. The elastic properties (Young's – *E*, and Shear modulus - *G*) are also significantly lower for the Fe based NbC grades. However, the lower elastic property values (*E* and *G*) indicate lower thermal stresses between the carbide and metal phases.

The microstructure and XRD results show the formation of a mixed carbide phase, (Nb,Mo)C, for the 4 wt% $Mo_2C$ additions to the NbC grades. The $Mo_2C$ additives form a solid solution with both the carbide and metal binder phases on sintering. In comparison, the addition of $Mo_2C$ to WC-Co results in η-phase formation in the WC and Co structure. The $Mo_2C$ additive shows a reduction of 52 % and 32 % in the mean NbC grain size for the Ni and Co binder grades, respectively. The addition of $Mo_2C$ has a negligible effect on the grain size of the NbC-Fe grade but influences the shape of the carbide grains as the grain morphology changes to more rounded or spherical particles.

In dry sliding wear at 700 °C, the NbC-Fe and NbC-FeNi have the lowest wear rates compared to the Ni and Co binders, and WC-Co. The wear rates of the NbC grades increases with the addition of $Mo_2C$ even though the coefficient of friction drops with $Mo_2C$ additions. Although $Mo_2C$ additives improves the room temperature hardness and assists with wetting of the NbC and metal binder during sintering, it has an adverse effect on the high temperature wear resistance of the NbC grades. This could be due to the tribo-oxidation processes at 700 °C, where $MoO_3$ most likely evaporates as $MoO_3$ becomes volatile above 600 °C. The Fe based binders without carbide additives show promise in high temperature wear applications at 700 °C. Further work is required to find additives which can improve the room temperature properties of NbC cermets with Fe and FeNi binders, and not have an adverse effect during high temperature wear.

## CRediT authorship contribution statement

**G. Peters:** Writing – review & editing, Writing – original draft, Methodology, Investigation. **D. Naidoo:** Writing – review & editing, Supervision. **R.M. Genga:** Writing – review & editing, Supervision, Conceptualization. **A. Shnier:** Writing – review & editing, Formal analysis. **S. Ngongo:** Formal analysis.

## Declaration of competing interest

The authors declare that they have no known competing financial interests or personal relationships that could have appeared to influence the work reported in this paper.

## Acknowledgements

The work was supported financially by the Department of Science and Innovation and the National Research Foundation, South Africa. The authors are grateful to Dr. Chris Freemantle and Pilot Tools (Pty) Ltd. for the use of their sintering facilities, hardness and density equipment. The authors are also grateful to BAM, Germany for the high temperature dry sliding wear tests, and to Prof. D. Billings for the use of the XRD facility at the University of the Witwatersrand.

## Data availability

Data will be made available on request.

## References

[1] J.H. Huang, S.G. Huang, P. Zhou, B. Lauwers, J. Qian, J. Vleugels, Microstructure and mechanical properties of WC or Mo2C modified NbC-Ni cermets, Int. J. Refract. Met. Hard Mater. 95 (2021), https://doi.org/10.1016/j.ijrmhm.2020.105440.
[2] A. Miyoshi, A. Hara, High temperature hardness of WC, TiC, TaC, NbC and their mixed carbides, J. Jpn. Soc. Powder Powder Metallurg. 12 (1965) 78–84, https://doi.org/10.2497/jjspm.12.78.
[3] M. Woydt, H. Mohrbacher, J. Vleugels, S. Huang, Niobium carbide for wear protection – tailoring its properties by processing and stoichiometry, Metal Powder Rep. 71 (2016) 265–272, https://doi.org/10.1016/j.mprp.2015.12.010.
[4] H.G. Schmidt, D. Marl, W. Benoit, C. Bonjour, The Mechanical Behaviour of Cemented Carbides at High Temperatures*, 1988.
[5] R.M. Genga, L.A. Cornish, M. Woydt, A. Janse van Vuuren, C. Polese, Microstructure, mechanical and machining properties of LPS and SPS NbC cemented carbides for face-milling of grey cast iron, Int. J. Refract. Met. Hard Mater. 73 (2018) 111–120, https://doi.org/10.1016/j.ijrmhm.2017.12.036.
[6] M. Labonne, J.-M. Missiaen, S. Lay, N. García, O. Lavigne, L.F. García, E. Tarrés, Sintering behavior and microstructural evolution of NbC-Ni cemented carbides with Mo2C additions, Int. J. Refract. Met. Hard Mater. 92 (2020) 105295, https://doi.org/10.1016/j.ijrmhm.2020.105295.
[7] S. Norgren, J. García, A. Blomqvist, L. Yin, Trends in the P/M hard metal industry, Int. J. Refract. Met. Hard Mater. 48 (2015) 31–45, https://doi.org/10.1016/j.ijrmhm.2014.07.007.
[8] D. Hübler, T. Gradt, Effect of different binders and secondary carbides on NbC cermets, Forschung Im Ingenieurwesen/Eng. Res. 86 (2022) 197–211, https://doi.org/10.1007/s10010-022-00583-1.
[9] S.G. Huang, L. Li, O. Van der Biest, J. Vleugels, Influence of WC addition on the microstructure and mechanical properties of NbC-Co cermets, J. Alloys Compd. 430 (2007) 158–164, https://doi.org/10.1016/j.jallcom.2006.05.015.
[10] S. Huang, P. De Baets, J. Sukumaran, H. Mohrbacher, M. Woydt, J. Vleugels, Effect of carbon content on the microstructure and mechanical properties of NbC-Ni based cermets, Metals (Basel) 8 (2018), https://doi.org/10.3390/met8030178.
[11] M. Woydt, H. Mohrbacher, The Background for the Use of Hartmetals and MMCs Based on Niobium Carbide (NbC) as Cutting Tools and for Wear Resistant Tribosystems. https://api.semanticscholar.org/CorpusID:55108570, 2015.
[12] M. Woydt, H. Mohrbacher, The tribological and mechanical properties of niobium carbides (NbC) bonded with cobalt or Fe3Al, Wear 321 (2014) 1–7, https://doi.org/10.1016/j.wear.2014.09.007.
[13] M. Woydt, H. Mohrbacher, The use of niobium carbide (NbC) as cutting tools and for wear resistant tribosystems, Int. J. Refract. Met. Hard Mater. 49 (2015) 212–218, https://doi.org/10.1016/j.ijrmhm.2014.07.002.
[14] M. Woydt, S. Huang, J. Vleugels, H. Mohrbacher, E. Cannizza, Potentials of niobium carbide (NbC) as cutting tools and for wear protection, Int. J. Refract. Met. Hard Mater. 72 (2018) 380–387, https://doi.org/10.1016/j.ijrmhm.2018.01.009.
[15] W.D. Schubert, M. Fugger, B. Wittmann, R. Useldinger, Aspects of sintering of cemented carbides with Fe-based binders, Int. J. Refract. Met. Hard Mater. 49 (2015) 110–123, https://doi.org/10.1016/j.ijrmhm.2014.07.028.
[16] E. Bennett, L. Lay, R. Morrell, B. Roebuck, A National Measurement Good Practice Guide: Microstructural Measurements on Ceramics and Hardmetals Microstructural Measurements on Ceramics and Hardmetals. https://www.npl.co.uk/gpgs/microstructural-measurements-ceramics-hardmetals, 1997.
[17] T. Kresse, D. Meinhard, T. Bernthaler, G. Schneider, Hardness of WC-Co hard metals: preparation, quantitative microstructure analysis, structure-property relationship and modelling, Int. J. Refract. Met. Hard Mater. 75 (2018) 287–293, https://doi.org/10.1016/j.ijrmhm.2018.05.003.
[18] H. Mohrbacher, M. Woydt, J. Vleugels, S. Huang, Niobium Carbide, An innovative and sustainable high-performance material for tooling, friction and wear applications, in: Advances in Materials Science for Environmental and Energy Technologies V, John Wiley & Sons, Ltd, 2016, pp. 67–80, https://doi.org/10.1002/9781119323624.ch7.
[19] J.K. Lancaster, The influence of substrate hardness on the formation and endurance of molybdenum disulphide films, Wear 10 (1967) 103–117, https://doi.org/10.1016/0043-1648(67)90082-8.
[20] S.G. Huang, J. Vleugels, H. Mohrbacher, M. Woydt, NbC grain growth control and mechanical properties of Ni bonded NbC cermets prepared by vacuum liquid phase sintering, Int. J. Refract. Met. Hard Mater. 72 (2018) 63–70, https://doi.org/10.1016/j.ijrmhm.2017.12.013.
[21] H. Moon, B.-K. Kim, S.-J.L. Kang, Growth mechanism of round-edged NbC grains in Co liquid, Acta Mater. 49 (2001) 1293–1299, https://doi.org/10.1016/S1359-6454(00)00394-3.
[22] J.P. Guha, D. Kolar, Systems of niobium monocarbide with transition metals, J. Less Common Metals 29 (1972) 33–40, https://doi.org/10.1016/0022-5088(72)90145-2.
[23] B. Wittmann, W.-D. Schubert, B. Lux, WC Grain Growth and Grain Growth Inhibition in Nickel and iron Binder Hardmetals, n.d. www.elsevier.com/locate/ijrmhm.
[24] S.G. Huang, J. Vleugels, H. Mohrbacher, M. Woydt, NbC-based cermets: influence of secondary carbide addition and metal binder, in: Proc. Int. Symp. on Wear Resistant Alloys for the Mining and Processing Industry, 2015.
[25] A.F. Guillermet, Thermodynamic properties of the Co-W-C system, Metall. Trans. A. 20 (1989) 935–956, https://doi.org/10.1007/BF02651660.
[26] A. Markström, B. Sundman, K. Frisk, A revised thermodynamic description of the Co-W-C system, J. Phase Equilib. Diffus. 26 (2005) 152–160, https://doi.org/10.1361/15477030522473.
[27] X. Li, X. Zhang, J. Zhang, Q. Zhang, V. Ji, J. Liu, Effect of Mo and C additions on eta phase evolution of WC-13Co cemented carbides, Coatings 12 (2022), https://doi.org/10.3390/coatings12121993.
[28] S.G. Huang, J. Vleugels, H. Mohrbacher, M. Woydt, Microstructure and tribological performance of NbC-Ni cermets modified by VC and Mo2C, Int. J. Refract. Met. Hard Mater. 66 (2017) 188–197, https://doi.org/10.1016/j.ijrmhm.2017.03.012.
[29] T.W. Penrice, Alternative Binders for Hard Metals, Springer-Verlag, New York Inc, 1987.
[30] S. Sheikh, R. M'Saoubi, P. Flasar, M. Schwind, T. Persson, J. Yang, L. Llanes, Fracture toughness of cemented carbides: testing method and microstructural effects, Int. J. Refract. Met. Hard Mater. 49 (2015) 153–160, https://doi.org/10.1016/j.ijrmhm.2014.08.018.
[31] J. Pötschke, A. Vornberger, C. Berger, Enhancement of hardness in niobium carbide composites, 2018.
[32] J.M. Tarragó, C. Ferrari, B. Reig, D. Coureaux, L. Schneider, L. Llanes, Mechanics and mechanisms of fatigue in a WC-Ni hardmetal and a comparative study with respect to WC-Co hardmetals, Int. J. Fatigue 70 (2015) 252–257, https://doi.org/10.1016/j.ijfatigue.2014.09.011.
[33] A. Chychko, J. García, V. Collado Ciprés, E. Holmström, A. Blomqvist, HV-KIC property charts of cemented carbides: a comprehensive data collection, Int. J. Refract. Met. Hard Mater. 103 (2022) 105763, https://doi.org/10.1016/j.ijrmhm.2021.105763.
[34] S.G. Huang, K. Vanmeensel, H. Mohrbacher, M. Woydt, J. Vleugels, Microstructure and mechanical properties of NbC-matrix hardmetals with secondary carbide addition and different metal binders, Int. J. Refract. Met. Hard Mater. 48 (2015) 418–426, https://doi.org/10.1016/j.ijrmhm.2014.10.014.
[35] S. Chao, N. Liu, Y. Yuan, C. Han, Y. Xu, M. Shi, J. Feng, Microstructure and mechanical properties of ultrafine Ti(CN)-based cermets fabricated from nano/submicron starting powders, Ceram. Int. 31 (2005) 851–862, https://doi.org/10.1016/j.ceramint.2004.09.013.
[36] R.M. Genga, P. Rokebrand, L.A. Cornish, N. Nelwalani, G. Brandt, N. Kelling, M. Woydt, A.J. van Vuuren, C. Polese, High-temperature sliding wear, elastic modulus and transverse rupture strength of Ni bonded NbC and WC cermets, Int. J. Refract. Met. Hard Mater. 87 (2020), https://doi.org/10.1016/j.ijrmhm.2019.105143.
[37] M. Woydt, H. Mohrbacher, The tribological property profile of hard metals and metal matrix composites based on niobium carbide, in: Proceedings of the International Symposium on Wear Resistant Alloys for the Mining and Processing Industry, Sao Paulo, Brazil, 2018, pp. 427–461.
[38] J. Yi, S. Xie, L. Chen, D. Yan, Influence of AlN addition on the microstructure, mechanical properties and oxidation characteristics of NbC-Ni cermets, Int. J. Refract. Met. Hard Mater. 118 (2024), https://doi.org/10.1016/j.ijrmhm.2023.106426.
[39] S.G. Huang, J. Vleugels, H. Mohrbacher, M. Woydt, Densification and tribological profile of niobium oxide, Wear 352–353 (2016) 65–71, https://doi.org/10.1016/j.wear.2016.02.003.
[40] M. Hadi, S.M. Rafiaei, F. Fernandes, The effect of Mo2C additions on the oxidation resistance of (Ti,W)CN cermets as base material for the production of cutting tools, Ceram. Int. 49 (2023) 21538–21545, https://doi.org/10.1016/j.ceramint.2023.03.288.
[41] Z. Anwer, C. Liu, B.L. Liu, R.M. Genga, J. Vleugels, S. Huang, A comparative study on the oxidation behaviour of NbC-Ni, WC-Co, and high entropy carbide-Ni based cermets, Int. J. Refract. Met. Hard Mater. 124 (2024) 106832, https://doi.org/10.1016/j.ijrmhm.2024.106832.
[42] M. Simnad, A. Spilners, Kinetics and mechanism of the oxidation of molybdenum, JOM 7 (1955) 1011–1016, https://doi.org/10.1007/BF03377603.